Am J Cancer Res 2025;15(6):2579-2594
www.ajcr.us /ISSN:2156-6976/ajcr0164979

Original Article

Correlation and predictive modeling of serum exosomal miRNAs and serological biomarkers for lymph node metastasis in gastric cancer

Quandong Li[1], Fang Nie[2], Dezhi Huang[1], Yongping Lin[1], Junjie Wan[1]

[1]National Cancer Center/National Clinical Research Center for Cancer/Cancer Hospital & Shenzhen Hospital, Chinese Academy of Medical Sciences and Peking Union Medical College, Shenzhen 518116, China; [2]Chengdu Second People's Hospital, Chengdu 610017, Sichuan, China

Received April 1, 2025; Accepted May 26, 2025; Epub June 15, 2025; Published June 30, 2025

Abstract: Objective: To evaluate the predictive potential of serum exosomal microRNAs (miRNAs) and traditional serological biomarkers for lymph node metastasis in gastric cancer and to assess their applicability in clinical practice. Methods: This retrospective study included 845 gastric cancer patients treated between January 2020 and December 2023, as the training cohort. Patients were stratified into lymph node-positive (n = 231) and lymph node-negative (n = 614) groups based on postoperative pathological evaluation. Serum exosomal miRNAs and conventional serological biomarkers were quantified and compared between groups. Multivariate logistic regression analysis was conducted to identify independent predictors. Model performance was validated using an independent test cohort comprising 277 patients (74 lymph node-positive, 203 lymph node-negative). Results: Patients with lymph node metastasis exhibited significantly elevated expression of miR-21, miR-20a, miR-27a, and miR-106a. Serological markers that were significantly higher in the lymph node positive group included carbohydrate antigen 724, carcinoembryonic antigen, hepatocyte growth factor, vascular endothelial growth factor, interleukin-6, and circulating cell-free DNA (all $P < 0.05$). A combined predictive model integrating both miRNA and serological data demonstrated strong diagnostic performance, with an area under the curve of 0.816 in the training cohort and 0.817 in the validation cohort. Conclusion: Serum exosomal miRNAs and serological biomarkers are significantly associated with lymph node metastasis in gastric cancer.

Keywords: Gastric cancer, lymph node metastasis, serum exosome miRNA, serological biomarkers, prediction model, cancer prognosis

Introduction

Gastric cancer remains a major global health concern, ranking as the fifth most common malignancy and the third leading cause of cancer-related mortality worldwide [1]. Its high mortality is largely due to late-stage diagnosis, with lymph node metastasis serving as a key determinant of disease progression and prognosis [2, 3]. Lymph node involvement not only indicates a poor prognosis but also critically influences treatment decisions. Current diagnostic methods for evaluating lymph node metastasis-primarily imaging and histopathological examination-are effective but limited by suboptimal sensitivity and specificity [4, 5].

Recent research has focused on identifying novel biomarkers that reflect early metastatic changes and can enhance diagnostic accuracy and prognostication [6, 7]. This study investigates miR-21, miR-20a, miR-27a, miR-106a, carbohydrate antigen 724 (CA724), carcinoembryonic antigen (CEA), hepatocyte growth factor (HGF), vascular endothelial growth factor (VEGF), interleukin-6 (IL-6) and circulating cell-free DNA (cfDNA), selected for their established roles in tumorigenesis, invasion, and metastasis [8, 9]. For example, miR-21 promotes epithelial-mesenchymal transition by targeting the PTEN/PI3K/AKT pathway, while CEA contributes to cancer cell adhesion and migration [9]. Together, these markers offer a multifaceted view of metastatic processes.

https://doi.org/10.62347/AOJE4206

The key innovation of this study lies in combining serum exosomal miRNAs with conventional serological biomarkers to construct a predictive model for lymph node metastasis. This integrative approach aims to capture both molecular and phenotypic characteristics of tumor progression, thereby improving predictive accuracy. Moreover, the model is validated on a large patient cohort, addressing limitations of previous studies that were constrained by small sample sizes and inconsistent methodologies.

Among novel biomarker candidates, serum exosomal miRNAs have gained substantial attention [10, 11]. Exosomes-extracellular vesicles involved in intercellular communication-carry stable miRNAs that are protected from enzymatic degradation. These miRNAs have been shown to correlate with clinical parameters such as tumor stage and metastatic status, highlighting their potential as minimally invasive biomarkers for predicting lymph node involvement [12, 13]. However, their application in gastric cancer remains insufficiently explored, and most available studies suffer from limited sample sizes and methodological variability.

Concurrently, traditional serological biomarkers have long been employed in gastric cancer management [14]. Common markers such as CEA and carbohydrate antigen 19-9 (CA19-9) are widely used in clinical practice but lack adequate sensitivity and specificity for detecting lymph node metastasis [15, 16]. Integrating these conventional biomarkers with molecular profiles like miRNAs may yield a more comprehensive and accurate assessment of metastatic risk [17, 18]. This approach is consistent with the broader movement toward personalized medicine, which emphasizes tailoring diagnosis and treatment based on individual molecular characteristics.

The development of robust predictive models based on multiple biomarkers requires rigorous statistical and computational methodologies. Correlation analysis facilitates identification of associations between exosomal miRNAs, serological markers, and lymph node metastasis. Advanced modeling techniques, including machine learning algorithms, can capture complex nonlinear relationships and improve predictive performance [7, 19]. Despite encouraging progress, challenges remain in terms of data heterogeneity, model interpretability, and clinical translation [20].

This study aims to address these gaps by conducting a comprehensive correlation and predictive modeling analysis of serum exosomal miRNAs and traditional serological biomarkers in relation to lymph node metastasis in gastric cancer. The ultimate goal is to establish a more effective, non-invasive tool to support early diagnosis and personalized therapeutic strategies, thereby improving clinical outcomes for gastric cancer patients.

Materials and methods

Patient selection

A retrospective analysis was conducted on 845 patients with gastric cancer treated at the National Cancer Center/National Clinical Research Center for Cancer/Cancer Hospital & Shenzhen Hospital, Chinese Academy of Medical Sciences and Peking Union Medical College between January 2020 and December 2023. These patients comprised the training set. Based on postoperative pathological evaluation of lymph node metastasis, patients were categorized into two groups: lymph node positive (n = 231) and lymph node negative (n = 619). An additional cohort of 277 patients meeting the same inclusion and exclusion criteria was used as an external test set for validation, with 74 cases in the lymph node positive group and 203 in the lymph node negative group. Patient data, including demographics, baseline characteristics, circulating exosomal miRNA levels, and serum biomarker profiles, were extracted from the hospital's electronic medical record system.

This study was designed as a retrospective cohort study. Data were obtained from the institutional medical records. The study protocol was reviewed and approved by the ethics committee of the aforementioned institution.

Inclusion criteria: (i) Age ≥ 18 years; (ii) Histopathological confirmation of gastric cancer with a definitive postoperative pathological report [21]; (iii) No chemotherapy, radiotherapy, or targeted therapy prior to serum [22]; (iv) Availability of complete and accurate clinical data.

Exclusion criteria: (i) Diagnosis of other malignancies; (ii) Presence of multiple distant metastases from gastric cancer; (iii) Pregnancy or lactation; (iv) Severe organ dysfunction (e.g., hepatic, renal), immune disorders, or systemic infections; (v) Poor physical status precluding surgery; (vi) Diagnosed neurological or psychiatric disorders affecting cognition or mental status.

Data extraction

Clinical data were extracted from the hospital's medical record system, including demographic variables (age, body mass index, smoking and alcohol history, comorbidities, education level, marital status), as well as tumor size and location.

The choice of surgical procedure was based on each patient's clinical status. Resected specimens were processed using standard histopathological techniques, including fixation, dehydration, clearing, paraffin embedding, and sectioning. Sections were stained with hematoxylin and eosin (H&E) for microscopic evaluation to determine tumor location, size, depth of invasion, and the presence of vascular or perineural invasion. Lymph nodes were serially sectioned and assessed for metastasis using H&E staining, periodic acid-Schiff (PAS) staining, and immunohistochemistry [23].

Circulating exosomal miRNA analysis: Within 24 hours of hospital admission, 5 mL of fasting venous blood was collected from each patient using tubes with or without clot activators. Samples were allowed to clot at room temperature for 10-60 minutes and centrifuged at 1,500×g for 20 minutes at 4°C using a high-speed refrigerated centrifuge (Eppendorf 5427R, Eppendorf China Co., Ltd.) to separate serum. The supernatant was transferred to a 1.5 mL centrifuge tube and centrifuged again at 3,000×g for 15 minutes at 4°C. The final serum supernatant was aliquoted and stored at -80°C under aseptic conditions.

A 500 μL aliquot of serum was used for exosome isolation using the Ribo™ Exosome Isolation Reagent (for plasma/serum). Exosomal markers CD63 and CD9, and the negative marker calnexin, were detected by enzyme-linked immunosorbent assay (ELISA) (Thermo MK3, Thermo Fisher Scientific, China). Serum exosomes were lysed with PIPA buffer, centrifuged at 21,100×g for 5 minutes, and the supernatant was subjected to 12% SDS-PAGE. Proteins were transferred to PVDF membranes at 100 mA for 2 hours, blocked with 1% BSA for 1 hour at room temperature, and incubated overnight at 4°C with primary antibodies (1:1,000 dilution). After three washes with TBST (5 minutes each), membranes were incubated for 1 hour at room temperature with HRP-conjugated goat anti-mouse IgG (1:2,000 dilution), followed by additional TBST washes and ECL detection.

miRNA expression was quantified via quantitative reverse transcription PCR (qRT-PCR). Total RNA was extracted using the exoRNeasy Serum/Plasma Midi Kit (Qiagen, Germany). Reverse transcription was performed with the TaqMan™ MicroRNA Reverse Transcription Kit and specific stem-loop primers (Applied Biosystems, Thermo Fisher Scientific, USA). The reverse transcription reaction included: 5 μL RNA, 2 μL 10× reverse transcription buffer, 0.25 μL dNTP (100 mmol/L), 4 μL reverse transcription primers (1 μmol/L), 0.5 μL reverse transcriptase (50 U/μL), 0.25 μL RNase inhibitor (20 U/μL), and 12 μL RNase-free water. The reaction conditions were 16°C for 30 minutes, 42°C for 30 minutes, and 85°C for 5 minutes. qPCR was performed using the TaqMan™ Universal PCR Master Mix with a 20 μL reaction mixture: 10 μL 2× Master Mix, 1 μL TaqMan™ probe, 1 μL reverse transcription product, and 8 μL RNase-free water.

Thecycling conditions were 95°C for 10 minutes, followed by 40 cycles of 95°C for 15 seconds and 60°C for 60 seconds. Relative miRNA expression levels were calculated using the 2^(-ΔΔCt) method.

Serum biomarkers: Fasting venous blood samples were collected within 24 hours of hospital admission. Serum was separated by centrifuging the blood at 3,000 rpm for 10 minutes at 4°C using a high-speed refrigerated centrifuge (TLD 12A, Hunan Xiangxi Scientific Instrument Factory, China). Biomarker quantification was performed using a magnetic immunoassay analyzer (Model M16, Shenzhen Bosheng Diagnostic Technology Co., Ltd., China).

ELISA were employed to quantify the following serum biomarkers: CA724 (Human CA72-4

ELISA Kit, Wuhan FineBiotech Co., Ltd., China); CA19-9 (Human CA19-9 ELISA Kit, Wuhan FineBiotech Co., Ltd., China); AFP (Human Alpha-Fetoprotein ELISA Kit, Abcam, UK); CEA (Human Carcinoembryonic Antigen ELISA Kit, Abcam, UK); HGF (Human HGF ELISA Kit, R&D Systems, USA); VEGF (Human VEGF Quantikine ELISA Kit, R&D Systems, USA); IL-6 and IL-8 (Quantikine ELISA Kits, R&D Systems, USA); Ferritin (Human Ferritin ELISA Kit, Abcam, UK).

Transferrin saturation was calculated based on serum iron and total iron-binding capacity (TIBC) using the Iron and TIBC Assay Kits (Abnova, Taiwan).

Additionally, concentrations of soluble ICAM-1 and E-selectin were measured using commercially available sandwich ELISA kits based on dual monoclonal antibodies (R&D Systems Europe, Abingdon, UK), following the manufacturer's instructions.

cfDNA was analyzed using the Oncomine cfDNA Assay Kit (Thermo Fisher Scientific, USA), with 10 mL of EDTA-anticoagulated whole blood as the input. cfDNA was extracted using the MagMAX cfDNA Isolation Kit (Thermo Fisher Scientific, USA; catalog number A29319) per manufacturer's protocol.

Following extraction, cfDNA was combined with pre-prepared primer/enzyme mixes. PCR thermocycling included initial denaturation, amplification, and final elongation. Unbound primers and contaminants were removed using magnetic bead or column-based purification, yielding clean amplicon libraries.

Library DNA concentration was quantified using a Qubit fluorometer (Thermo Fisher Scientific, USA), and fragment length was assessed via TapeStation (Agilent Technologies, USA) to ensure quality. Libraries were adjusted to meet the loading requirements of the Ion GeneStudio S5 sequencing system (Thermo Fisher Scientific, USA), with the appropriate chip selected based on expected throughput. Libraries were then loaded onto the sequencer, and cfDNA sequencing was carried out following the manufacturer's protocol.

Outcome measures

The primary objectives were to (i) assess the diagnostic performance of individual and combined biomarkers and (ii) validate their clinical applicability.

First, statistical analyses were conducted to identify exosomal miRNAs and serological biomarkers significantly associated with lymph node metastasis. Next, a combined predictive model integrating both biomarker types was developed and externally validated. Positive predictive value (PPV) and negative predictive value (NPV) were calculated to further assess clinical utility. These analyses contribute to model optimization and support its generalizability across diverse patient populations.

Statistical analysis

Statistical analyses were performed using SPSS version 29.0 (SPSS Inc., Chicago, IL, USA). Continuous variables were expressed as mean ± standard deviation or median with interquartile range, depending on the data distribution. Categorical variables were summarized using frequencies and percentages.

Comparisons between two groups for continuous variables were performed using independent-sample t-tests and Chi-square tests for categorical variables. Multivariate logistic regression was used to calculate odds ratios (ORs) and 95% confidence intervals (CIs) for potential predictors treated as continuous variables.

Correlation analyses were conducted using Pearson correlation for normally distributed continuous variables and Spearman correlation for ordinal or non-normally distributed data. A two-sided p-value < 0.05 was considered statistically significant.

Results

Comparison of demographic and baseline characteristics in the training set

No statistically significant differences were observed between the lymph node positive and the lymph node negative groups in terms of age, sex, body mass index, smoking history, alcohol use, hypertension, diabetes, education level, marital status, or ethnicity (all P > 0.05) (**Table 1**).

However, significant differences were found in tumor-related characteristics. Tumor location differed between groups (χ^2 = 13.543, P =

Table 1. Comparison of demographic and baseline characteristics in the training set

	Lymph Node Positive group (n = 231)	Lymph Node Negative group (n = 614)	t/χ^2	P
Age (years)	59.85 ± 2.65	60.21 ± 2.97	1.694	0.091
Female/Male	127 (54.98%)/104 (45.02%)	380 (61.89%)/234 (38.11%)	3.34	0.068
Body Mass Index (kg/m^2)	23.51 ± 1.35	23.49 ± 1.47	0.142	0.887
Smoking history (Yes/No)	89 (38.53%)/142 (61.47%)	251 (40.88%)/363 (59.12%)	0.386	0.534
Drinking history (Yes/No)	61 (26.41%)/170 (73.59%)	154 (25.08%)/460 (74.92%)	0.155	0.693
Hypertension (Yes/No)	41 (17.75%)/190 (82.25%)	135 (21.99%)/479 (78.01%)	1.828	0.176
Diabetes (Yes/No)	49 (21.21%)/182 (78.79%)	163 (26.55%)/451 (73.45%)	2.542	0.111
Educational level (Junior college graduate or lower/College graduate or higher)	61 (26.41%)/170 (73.59%)	174 (28.34%)/440 (71.66%)	0.312	0.576
Marital Status (Married/Unmarried)	204 (88.31%)/27 (11.69%)	553 (90.07%)/61 (9.93%)	0.553	0.457
Ethnicity (Han/Other)	59.85 ± 2.65	60.21 ± 2.97	1.694	0.091
Tumor length (> 2 cm/≤ 2 cm)	127 (54.98%)/104 (45.02%)	380 (61.89%)/234 (38.11%)	3.340	0.068
Tumor location			13.543	0.001
Upper Stomach	6 (2.6%)	64 (10.42%)		
Middle Stomach	47 (20.35%)	113 (18.4%)		
Lower Stomach	178 (77.06%)	437 (71.17%)		
Tumor Invasion Depth (Submucosa /Mucosa)	184 (79.65%)/47 (20.35%)	306 (49.84%)/308 (50.16%)	61.253	< 0.001
Vascular Invasion (Yes/No)	137 (59.31%)/94 (40.69%)	254 (41.37%)/360 (58.63%)	21.728	< 0.001
Perineural Invasion (Yes/No)	216 (93.51%)/15 (6.49%)	268 (43.65%)/346 (56.35%)	170.514	< 0.001
Tumor Differentiation			9.118	0.010
Poorly Differentiated	122 (52.81%)	314 (51.14%)		
Moderately Differentiated	79 (34.2%)	168 (27.36%)		
Well Differentiated	30 (12.99%)	132 (21.5%)		

0.001), with a higher proportion of lower stomach tumors and fewer upper stomach tumors in the lymph node positive group. Tumor invasion depth also varied markedly (χ^2 = 61.253, P < 0.001), with deeper submucosal invasion more prevalent in the lymph node positive group. Additionally, vascular invasion (χ^2 = 21.728, P < 0.001) and perineural invasion (χ^2 = 170.514, P < 0.001) were significantly more frequent in patients with lymph node positive group. Tumor differentiation showed significant group differences (χ^2 = 9.118, P = 0.01), with poorly differentiated tumors slightly more common in the positive group.

Comparison of serum exosomal miRNAs between lymph node positive and lymph node negative groups in the training set

Patients with lymph node metastasis exhibited significantly higher levels of miR-21 (5.36 ± 0.59 vs. 5.21 ± 0.64; t = 3.215, P = 0.001), miR-20a (2.44 ± 0.45 vs. 2.36 ± 0.23; t = 2.483, P = 0.014), miR-27a (2.02 ± 0.62 vs. 1.88 ± 0.58; t = 3.231, P = 0.001), and miR-106a (41.65 ± 9.21 vs. 39.65 ± 8.64; t = 2.94, P = 0.003), compared to those without metastasis (**Figure 1**).

Comparison of serum biomarkers in the training set

Compared with the lymph node negative group, the lymph node positive group showed significantly elevated levels of the following biomarkers.

CA724 (39.41 ± 5.61 U/ml vs. 38.52 ± 5.56 U/ml; t = 2.083, P = 0.038), CA19-9 (50.65 ± 5.98 U/ml vs. 49.53 ± 5.12 U/ml; t = 2.533, P = 0.012), AFP (11.03 ± 2.11 ng/ml vs. 10.64 ± 2.71 ng/ml; t = 2.225, P = 0.026), CEA (20.65 ± 4.27 ng/ml vs. 19.77 ± 4.23 ng/ml; t = 2.677, P = 0.008), HGF (6.35 ± 2.21 pg/ml vs. 5.92 ± 1.41 pg/ml; t = 2.756, P = 0.006), and VEGF (368.32 ± 83.56 ng/L vs. 350.15 ± 87.14 ng/L; t = 2.732, P = 0.006).

In contrast, the lymph node positive group had significantly lower levels of transferrin saturation (27.94 ± 4.84% vs. 29.08 ± 4.24%; t = 3.173, P = 0.002) and ferritin (87.2 ± 24.25 ng/mL vs. 91.47 ± 28.35 ng/mL; t = 2.173, P = 0.030).

Additionally, elevated levels of sE-Selectin (44.56 ± 5.78 ng/mL vs. 45.65 ± 5.29 ng/mL; t = 2.597, P = 0.010), sICAM-1 (245.84 ± 32.78 ng/mL vs. 237.37 ± 51.82 ng/mL; t = 2.818, P = 0.005), IL-6 (1.57 ± 0.41 pg/mL vs. 1.49 ± 0.26 pg/mL; t = 2.846, P = 0.005), IL-8 (61.85 ± 5.65 pg/mL vs. 60.69 ± 5.98 pg/mL; t = 2.554, P = 0.011), and cfDNA (103.54 ± 26.35 ng/mL vs. 99.32 ± 25.86 ng/mL; t = 2.105, P = 0.036) were also observed in the lymph node positive group (**Table 2**).

Multivariate logistic regression analysis of predictors for lymph node metastasis

Multivariate logistic regression analysis identified several circulating exosomal miRNAs and serum biomarkers as independent predictors of lymph node metastasis.

Among exosomal miRNAs included miR-21 (Coefficient: -0.454, P = 0.009, OR = 0.635, 95% CI: 0.451-0.894) and miR -20a (Coefficient: -0.697, P = 0.022, OR = 0.498, 95% CI: 0.275-0.903).

These were significantly associated with a reduced risk of lymph node metastasis, whereasmiR-27a and miR-106a did not show statistically significant associations (both P > 0.05).

Among serological markers, CEA (Coefficient: -0.051, P = 0.038, OR = 0.950, 95% CI: 0.905-0.997), HGF (Coefficient: -0.172, P = 0.003, OR = 0.842, 95% CI: 0.751-0.945), VEGF (Coefficient: -0.003, P = 0.027, OR = 0.997, 95% CI: 0.995-1.000), IL-6 (Coefficient: -0.936, P = 0.003, OR = 0.392, 95% CI: 0.211-0.730), and cfDNA (Coefficient: -0.010, P = 0.008, OR = 0.990, 95% CI: 0.982-0.997) showed inverse associations with lymph node metastasis.

In contrast, transferrin saturation (Coefficient: 0.075, P = 0.001, OR = 1.078, 95% CI: 1.030-1.128) and sE-Selectin (Coefficient: 0.051, P = 0.007, OR = 1.052, 95% CI: 1.014-1.092) were positively associated with metastasis risk. Other markers, including CA724, CA19-9, AFP, ferritin, sICAM-1, and IL-8, were not significantly associated (all P > 0.05) (**Table 3**).

Receiver operating characteristic (ROC) analysis in the training set

In the training cohort, a combined predictive model incorporating the selected serum exosomal miRNAs and serum biomarkers was con-

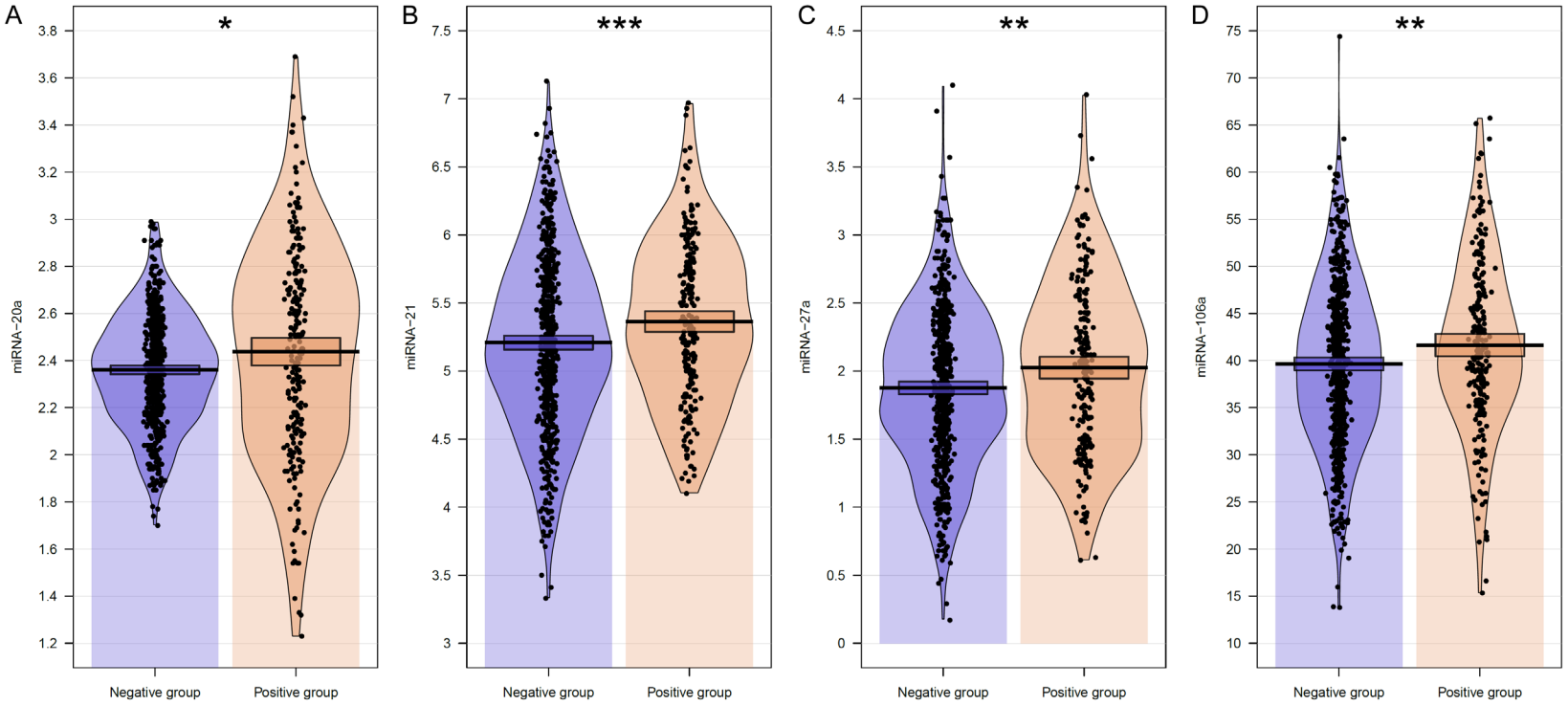

Figure 1. Comparison of serum exosomal miRNA between two groups in the training set. A: miRNA-20a; B: miRNA-21; C: miRNA-27a; D: miRNA-106a. *P < 0.05, **P < 0.01, ***P < 0.001.

Table 2. Comparison of serum biomarkers in the training set

	Lymph Node Positive group (n = 231)	Lymph Node Negative group (n = 614)	t	P
Ca724 (U/ml)	39.41 ± 5.61	38.52 ± 5.56	2.083	0.038
Ca199 (U/ml)	50.65 ± 5.98	49.53 ± 5.12	2.533	0.012
AFP (ng/ml)	11.03 ± 2.11	10.64 ± 2.71	2.225	0.026
CEA (ng/ml)	20.65 ± 4.27	19.77 ± 4.23	2.677	0.008
HGF (pg/ml)	6.35 ± 2.21	5.92 ± 1.41	2.756	0.006
VEGF (ng/L)	368.32 ± 83.56	350.15 ± 87.14	2.732	0.006
Transferrin saturation (%)	27.94 ± 4.84	29.08 ± 4.24	3.173	0.002
Ferritin (ng/ml)	87.2 ± 24.25	91.47 ± 28.35	2.173	0.030
sE-Selectin (ng/ml)	44.56 ± 5.78	45.65 ± 5.29	2.597	0.010
sICAM-1 (ng/ml)	245.84 ± 32.78	237.37 ± 51.82	2.818	0.005
IL-6 (pg/ml)	1.57 ± 0.41	1.49 ± 0.26	2.846	0.005
IL-8 (pg/ml)	61.85 ± 5.65	60.69 ± 5.98	2.554	0.011
cfDNA (ng/ml)	103.54 ± 26.35	99.32 ± 25.86	2.105	0.036

CA724: Carbohydrate Antigen 72-4; CA19-9: Carbohydrate Antigen 19-9; AFP: Alpha-Fetoprotein; CEA: Carcinoembryonic Antigen; HGF: Hepatocyte Growth Factor; VEGF: Vascular Endothelial Growth Factor; sE-Selectin: Soluble E-Selectin; sICAM-1: Soluble Intercellular Adhesion Molecule-1; IL-6: Interleukin-6; IL-8: Interleukin-8; cfDNA: Cell-Free DNA.

Table 3. Multivariate logistic regression analysis of lymph node metastasis in gastric cancer

	Coefficient	Std Error	Wald Stat	P	OR	OR CI Lower	OR CI Upper
miRNA-21 level	-0.454	0.175	-2.600	0.009	0.635	0.451	0.894
miRNA-20a level	-0.697	0.303	-2.297	0.022	0.498	0.275	0.903
miRNA-27a level	-0.265	0.172	-1.545	0.122	0.767	0.548	1.074
miRNA-106a level	-0.019	0.011	-1.699	0.089	0.981	0.959	1.003
Ca724 (U/ml)	-0.018	0.019	-0.958	0.338	0.982	0.946	1.019
Ca199 (U/ml)	-0.035	0.019	-1.858	0.063	0.966	0.931	1.002
AFP (ng/ml)	-0.065	0.042	-1.558	0.119	0.937	0.864	1.017
CEA (ng/ml)	-0.051	0.025	-2.079	0.038	0.950	0.905	0.997
HGF (pg/ml)	-0.172	0.059	-2.928	0.003	0.842	0.751	0.945
VEGF (ng/L)	-0.003	0.001	-2.208	0.027	0.997	0.995	1.000
Transferrin saturation (%)	0.075	0.023	3.215	0.001	1.078	1.030	1.128
Ferritin (ng/ml)	0.007	0.004	1.753	0.080	1.007	0.999	1.014
sE-Selectin (ng/ml)	0.051	0.019	2.700	0.007	1.052	1.014	1.092
sICAM-1 (ng/ml)	-0.004	0.002	-1.823	0.068	0.996	0.992	1.000
IL-6 (pg/ml)	-0.936	0.317	-2.952	0.003	0.392	0.211	0.730
IL-8 (pg/ml)	-0.030	0.018	-1.715	0.086	0.970	0.937	1.004
cfDNA (ng/ml)	-0.010	0.004	-2.658	0.008	0.990	0.982	0.997

structed to assess the risk of lymph node metastasis in gastric cancer. The model demonstrated strong discriminative performance, with an area under the ROC curve (AUC) of 0.816, indicating good predictive accuracy (**Figure 2**).

Cut-off values and diagnostic performance indicators of serum exosomal miRNAs and serological biomarkers

The diagnostic performance of serum exosomal miRNAs and serological biomarkers in predicting lymph node metastasis in gastric cancer was evaluated (**Table 4**). Cut-off values, PPV, and NPV were calculated for each biomarker group. The optimal cut-off for serum exosomal miRNAs was 0.645, yielding a PPV of 57.61% and an NPV of 87.15%. For serological biomarkers, the cut-off value was 0.683, with a notably higher PPV of 70.47% and an NPV of 93.75%.

These results suggest that while both biomarker types demonstrated predictive value, serum

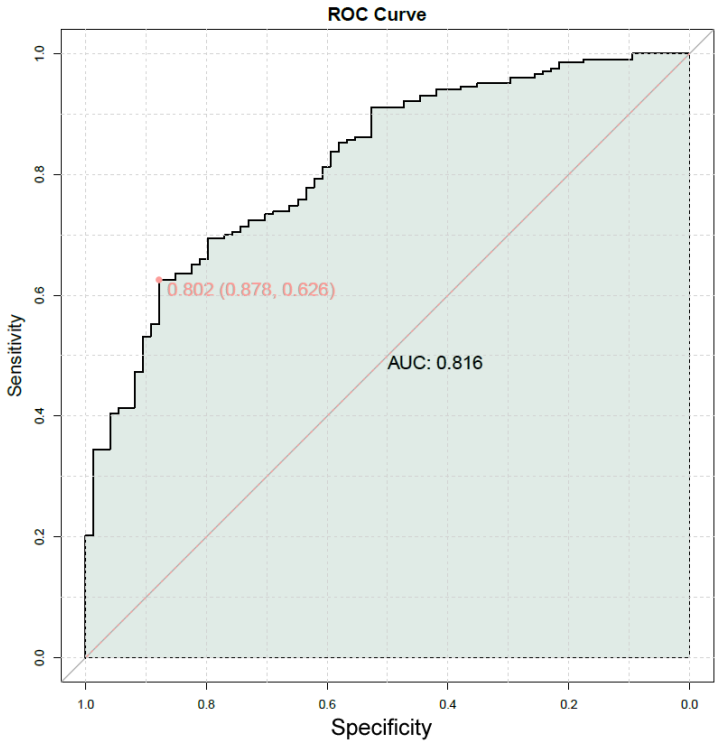

Figure 2. ROC curve of lymph node metastasis in the training set.

Table 4. Cut-off values and diagnostic performance indicators for serum exosomal mirnas and serological biomarkers

	Cut-off Value	PPV	NPV
Serum Exosome miRNA	0.645	57.61%	87.15%
Serum Biological Markers	0.683	70.47%	93.75%

PPV: positive predictive value; NPV: negative predictive value.

biomarkers exhibited superior diagnostic performance. Specifically, their higher PPV reflects a stronger ability to correctly identify patients with lymph node metastasis, while the high NPV indicates greater reliability in excluding metastasis. These findings underscore the potential clinical utility of serum biomarkers in risk stratification and management of gastric cancer. Future studies with larger independent cohorts are warranted to validate and refine these diagnostic thresholds.

Comparison of demographic and baseline characteristics in the test set

No significant differences were observed between the lymph node positive and lymph node negative groups in terms of age, sex, body mass index, smoking and alcohol history, hypertension, diabetes, educational level, marital status, or ethnicity (all $P > 0.05$) (**Table 5**).

However, significant differences were noted in tumor characteristics. The lymph node positive group had a higher proportion of tumors > 2 cm (74.32% vs. 41.38%; $\chi^2 = 23.545$, $P < 0.001$), greater depth of invasion (82.43% vs. 50.25%; $\chi^2 = 23.198$, $P < 0.001$), and a higher incidence of perineural invasion (83.78% vs. 53.69%; $\chi^2 = 20.784$, $P < 0.001$). Tumor differentiation also significantly differed between groups ($\chi^2 = 6.219$, $P = 0.045$), with poorly differentiated tumors more common in the lymph node positive group. No significant differences were observed in tumor location or vascular invasion ($P > 0.05$). These results reinforce the relevance of specific tumor features in predicting lymph node metastasis.

Comparison of serum exosomal miRNAs in the test set

Patients with lymph node metastasis in the test set exhibited significantly higher levels of: miR-21 (5.39 ± 0.43 vs. 5.26 ± 0.47; t = 2.189, P = 0.029), miR-20a (2.41 ± 0.63 vs. 2.25 ± 0.54; t = 2.084, P = 0.038), miR-27a (2.12 ± 0.52 vs. 1.95 ± 0.61; t = 2.185, P = 0.030), miR-106a (41.97 ± 15.87 vs. 38.03 ± 7.36; t = 2.055, P = 0.043) (**Figure 3**).

Comparison of serum biomarkers in the test set

The lymph node positive group showed significantly higher levels of: CA724 (40.41 ± 6.18 U/mL vs. 38.06 ± 5.86 U/mL; t = 2.910, P = 0.004); CA19-9 (49.88 ± 5.32 U/mL vs. 48.31 ± 5.61 U/mL; t = 2.089, P = 0.038); AFP (11.25 ± 2.35 ng/mL vs. 10.14 ± 2.54 ng/mL; t = 3.265, P = 0.001); CEA (20.83 ± 4.18 ng/mL vs. 19.49 ± 4.69 ng/mL; t = 2.150, P = 0.032); HGF (6.26 ± 2.41 pg/mL vs. 5.53 ± 1.65 pg/mL; t = 2.393, P = 0.019); VEGF (369.17 ± 89.56 pg/mL vs. 342.96 ± 86.65 pg/mL; t =

Table 5. Comparison of demographic and baseline characteristics in the test set

	Lymph Node Positive group (n = 74)	Lymph Node Negative group (n = 203)	t/χ^2	P
Age (years)	60.78 ± 1.76	60.94 ± 2.37	0.584	0.56
Female/Male	40 (54.05%)/34 (45.95%)	126 (62.07%)/77 (37.93%)	1.451	0.228
Body Mass Index (kg/m^2)	23.47 ± 1.42	23.45 ± 1.39	0.116	0.908
Smoking history (Yes/No)	29 (39.19%)/45 (60.81%)	83 (40.89%)/120 (59.11%)	0.065	0.799
Drinking history (Yes/No)	20 (27.03%)/54 (72.97%)	51 (25.12%)/152 (74.88%)	0.103	0.748
Hypertension (Yes/No)	13 (17.57%)/61 (82.43%)	48 (23.65%)/155 (76.35%)	1.167	0.28
Diabetes (Yes/No)	15 (20.27%)/59 (79.73%)	47 (23.15%)/156 (76.85%)	0.259	0.611
Educational level (Junior college graduate/College graduate or higher)	20 (27.03%)/54 (72.97%)	58 (28.57%)/145 (71.43%)	0.064	0.8
Marital Status (Married/Unmarried)	68 (91.89%)/6 (8.11%)	194 (95.57%)/9 (4.43%)	0.802	0.37
Ethnicity (Han/Other)	71 (95.95%)/3 (4.05%)	187 (92.12%)/16 (7.88%)	1.244	0.265
Tumor length (> 2 cm/≤ 2 cm)	55 (74.32%)/19 (25.68%)	84 (41.38%)/119 (58.62%)	23.545	< 0.001
Tumor location			4.168	0.124
Upper Stomach	2 (2.7%)	21 (10.34%)		
Middle Stomach	15 (20.27%)	37 (18.23%)		
Lower Stomach	57 (77.03%)	145 (71.43%)		
Tumor Invasion Depth (Submucosa /Mucosa)	61 (82.43%)/13 (17.57%)	102 (50.25%)/101 (49.75%)	23.198	< 0.001
Vascular Invasion (Yes/No)	45 (60.81%)/29 (39.19%)	104 (51.23%)/99 (48.77%)	2.002	0.157
Perineural Invasion (Yes/No)	62 (83.78%)/12 (16.22%)	109 (53.69%)/94 (46.31%)	20.784	< 0.001
Tumor Differentiation			6.219	0.045
Poorly Differentiated	39 (52.7%)	94 (46.31%)		
Moderately Differentiated	26 (35.14%)	56 (27.59%)		
Well Differentiated	9 (12.16%)	53 (26.11%)		

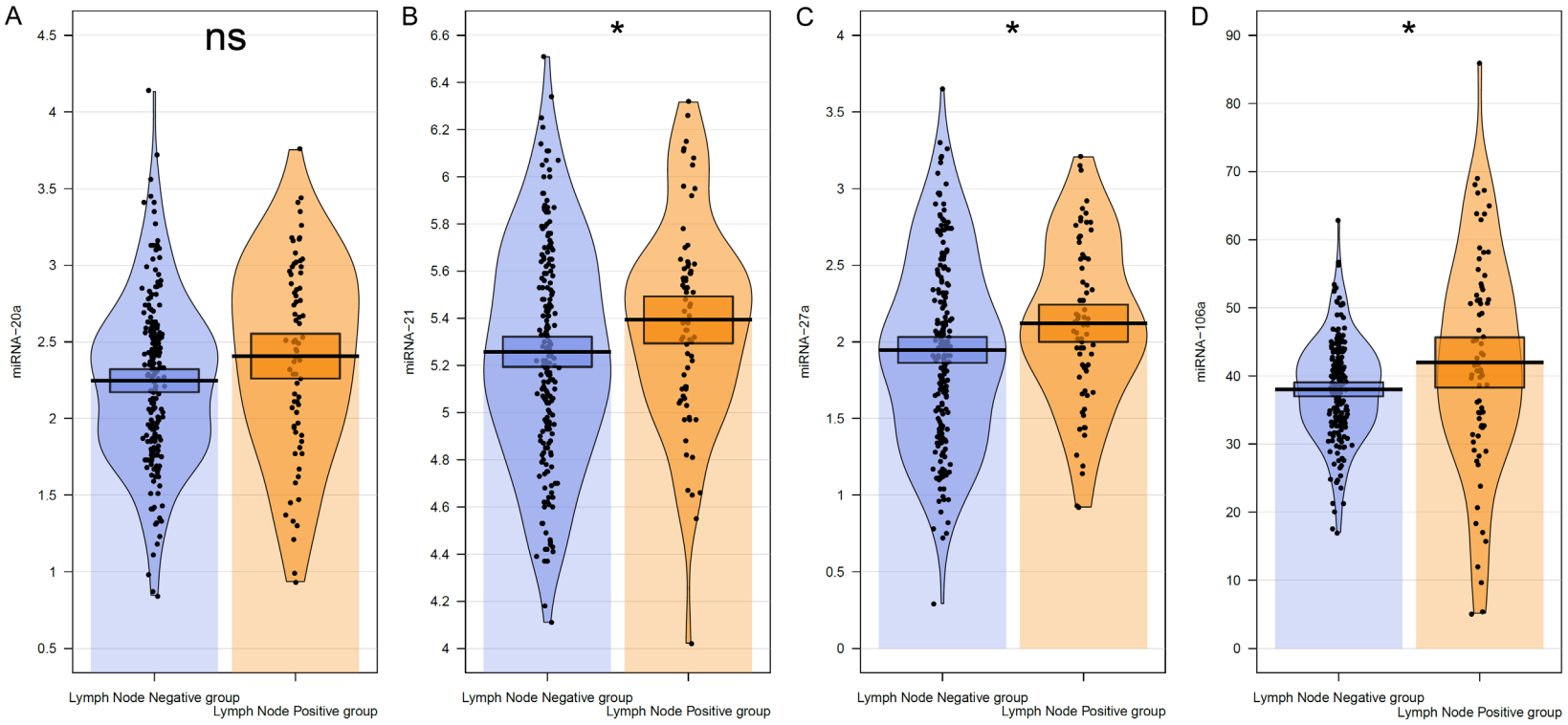

Figure 3. Comparison of serum exosomal miRNA in the test set. A: miRNA-20a; B: miRNA-21; C: miRNA-27a; D: miRNA-106a. ns: $P > 0.05$, *$P < 0.05$.

Table 6. Comparison of serum biomarkers in the test set

	Lymph Node Positive group (n = 74)	Lymph Node Negative group (n = 203)	t	P
Ca724 (U/ml)	40.41 ± 6.18	38.06 ± 5.86	2.91	0.004
Ca199 (U/ml)	49.88 ± 5.32	48.31 ± 5.61	2.089	0.038
AFP (ng/ml)	11.25 ± 2.35	10.14 ± 2.54	3.265	0.001
CEA (ng/ml)	20.83 ± 4.18	19.49 ± 4.69	2.15	0.032
HGF (pg/ml)	6.26 ± 2.41	5.53 ± 1.65	2.393	0.019
VEGF (pg/ml)	369.17 ± 89.56	342.96 ± 86.65	2.207	0.028
Transferrin saturation (%)	28.34 ± 4.65	30.14 ± 5.62	2.464	0.014
Ferritin (ng/ml)	86.12 ± 20.65	92.14 ± 25.63	2.008	0.046
sE-Selectin (ng/ml)	44.84 ± 5.38	46.29 ± 5.36	1.981	0.049
sICAM-1 (ng/ml)	248.89 ± 30.52	238.32 ± 50.65	2.104	0.037
IL-6 (pg/ml)	1.58 ± 0.34	1.46 ± 0.21	3.054	0.003
IL-8 (pg/ml)	61.91 ± 5.65	60.31 ± 5.32	2.178	0.030
cfDNA (ng/ml)	104.51 ± 25.68	97.55 ± 24.68	2.054	0.041

CA724: Carbohydrate Antigen 72-4; CA19-9: Carbohydrate Antigen 19-9; AFP: Alpha-Fetoprotein; CEA: Carcinoembryonic Antigen; HGF: Hepatocyte Growth Factor; VEGF: Vascular Endothelial Growth Factor; sE-Selectin: Soluble E-Selectin; sICAM-1: Soluble Intercellular Adhesion Molecule-1; IL-6: Interleukin-6; IL-8: Interleukin-8; cfDNA: Cell-Free DNA.

2.207, P = 0.028); sICAM-1 (248.89 ± 30.52 ng/mL vs. 238.32 ± 50.65 ng/mL; t = 2.104, P = 0.037); IL-6 (1.58 ± 0.34 pg/mL vs. 1.46 ± 0.21 pg/mL; t = 3.054, P = 0.003); IL-8 (61.91 ± 5.65 pg/mL vs. 60.31 ± 5.32 pg/mL; t = 2.178, P = 0.030); cfDNA (104.51 ± 25.68 ng/mL vs. 97.55 ± 24.68 ng/mL; t = 2.054, P = 0.041).

In contrast, the lymph node positive group had significantly lower levels of: Transferrin saturation (28.34 ± 4.65% vs. 30.14 ± 5.62%; t = 2.464, P = 0.014). Ferritin (86.12 ± 20.65 ng/mL vs. 92.14 ± 25.63 ng/mL; t = 2.008, P = 0.046). sE-Selectin (44.84 ± 5.38 ng/mL vs. 46.29 ± 5.36 ng/mL; t = 1.981, P = 0.049) (**Table 6**).

These results further validate the associations observed in the training set and highlight the relevance of these biomarkers for predicting lymph node metastasis in clinical practice.

ROC analysis in the test set

A combined predictive model incorporating serum exosomal miRNAs and serological biomarkers was tested in the independent validation cohort (test set). The model yielded an AUC of 0.817, indicating robust discriminatory ability for predicting lymph node metastasis in gastric cancer (**Figure 4**).

Discussion

Circulating exosomal miRNAs reflect the tumor's genetic profile and biological behavior, offering valuable insights into metastatic potential [24, 25]. In this study, elevated levels of miR-21, miR-20a, miR-27a, and miR-106a in patients with lymph node metastasis suggest their oncogenic roles.

miR-21 is well-known for promoting epithelial-mesenchymal transition and inhibiting apoptosis via modulation of the PTEN/PI3K/AKT pathway. This contributes to enhanced cell survival, invasiveness, and metastatic capacity. Additionally, miR-21 facilitates extracellular matrix remodeling and degradation, both critical for cancer dissemination [26].

Similarly, miR-20a promotes tumor progression by downregulating E2F1, thereby disrupting cell cycle control and promoting unchecked proliferation. It also suppresses TGF-β signaling, weakening tumor-suppressive mechanisms and facilitating invasiveness [27]. miR-27a plays a crucial role in angiogenesis regulation, particularly through the VEGF and angiopoietin signaling pathways, enabling tumor vascularization and systemic spread.

miR-106a, significantly upregulated in lymph node-positive patients, exerts its influence by targeting cell cycle regulators such as p21, a cyclin-dependent kinase inhibitor. This inhibition promotes cell cycle progression and proliferation [28]. Additionally, miR-106a may modulate immune evasion mechanisms, fostering an immunosuppressive microenvironment that favors metastasis. Collectively, the dysregula-

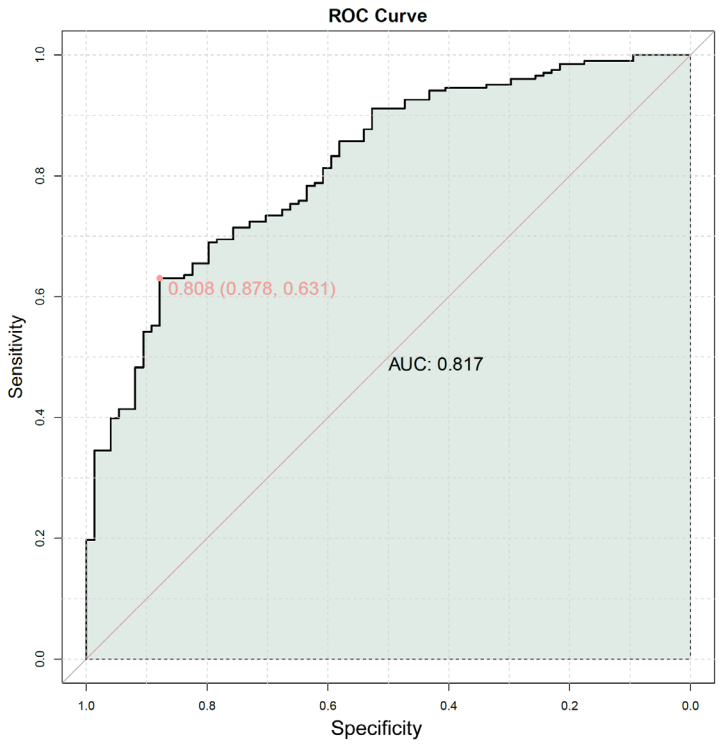

Figure 4. ROC curve of lymph node metastasis in the test set.

tion of these miRNAs underscores their functional roles as metastasis facilitators and highlights their potential as non-invasive diagnostic biomarkers in gastric cancer.

Turning to serological biomarkers, elevated levels of CA724, CA19-9, AFP, CEA, HGF, and VEGF in the lymph node positive group further emphasize their associations with tumor aggressiveness. CA724 and CA19-9 are established tumor markers in gastric cancer, and their upregulation reflects heightened tumor activity and metastatic potential [29, 30]. Although AFP is primarily associated with hepatocellular carcinoma, its elevation in gastric cancer may indicate aberrant protein expression linked to dedifferentiation and increased malignancy [31, 32].

CEA is a well-documented marker of metastatic potential, particularly due to its role in promoting cell adhesion, migration, and proliferation [33, 34]. Its ability to mediate interactions between tumor cells and the extracellular matrix is thought to facilitate metastatic spread. HGF and VEGF, both critical pro-angiogenic factors, support tumor vascularization and are closely tied to the mechanisms of invasion and dissemination [35, 36].

In particular, VEGF promotes both angiogenesis and lymphangiogenesis, which likely contributes to the increased risk of lymphatic spread observed in node-positive patients [37, 38]. HGF, through c-Met signaling, not only drives cell proliferation but also enhances cellular detachment from the primary tumor, facilitating metastatic transit [39].

Reduced levels of transferrin saturation and ferritin may reflect the high iron demand of rapidly proliferating tumor cells, consistent with a metabolic profile of aggressive disease [40].

Additionally, elevated levels of sE-Selectin, sICAM-1, IL-6, IL-8, and cfDNA further support the involvement of systemic and immune-mediated pathways in metastasis. Soluble adhesion molecules like sE-Selectin and sICAM-1 facilitate tumor cell attachment to the endothelium, aiding vascular arrest and lymphatic infiltration. sE-Selectin, in particular, interacts with selectin ligands on circulating tumor cells, enabling their entrapment in target tissues.

Proinflammatory cytokines such as IL-6 and IL-8 contribute to immune evasion and tumor progression by promoting inflammatory responses that favor tumor growth and suppress immune surveillance [41, 42]. IL-6 is particularly important, as it activates the JAK/STAT signaling pathway, enhancing tumor cell proliferation and resistance to immune-mediated destruction [43]. Lastly, increased circulating levels of cell-free DNA (cfDNA) suggest elevated cell turnover due to apoptosis and necrosis, features commonly observed in highly metastatic tumors [44].

Multivariate logistic regression analysis reinforces the relevance of both biomarker categories-exosomal miRNAs and serological factors-in reflecting the biological processes underlying metastasis. While miRNAs represent genetic-level alterations central to tumor progression, serological markers provide systemic insight into physiological responses to increasing tumor burden. Their combined predictive

capacity, as evidenced by high AUC values from ROC curve analysis, supports a novel and integrative model for assessing lymphatic dissemination risk.

This study offers valuable insights into the association between serum exosomal miRNAs, serological biomarkers, and lymph node metastasis in gastric cancer. However, further research is warranted to elucidate the dynamic interplay between these two biomarker types and to validate their prognostic utility in clinical settings. A key unresolved question is whether these biomarkers act merely as bystanders or as active drivers of metastasis. Establishing causality and understanding their mechanistic roles remain critical for advancing therapeutic applications.

Despite the strengths of our study, several limitations should be acknowledged. The retrospective design introduces potential selection bias, and the single-center setting may limit the generalizability of the findings. Although the sample size is relatively large, it may not fully capture population-level heterogeneity. Additionally, we did not account for potential confounding variables such as genetic polymorphisms or environmental factors that may influence biomarker expression. Importantly, our study demonstrates associations rather than causative relationships between these biomarkers and metastasis. Prospective, multicenter studies combined with mechanistic investigations are necessary to validate these findings and facilitate clinical translation.

Conclusion

In summary, this study highlights key molecular and systemic contributors to lymph node metastasis in gastric cancer, notably involving specific exosomal miRNAs and serum-based biomarkers. The integration of these biomarkers enhances our understanding of metastatic mechanisms and contributes to the development of robust predictive models. These findings position the investigated biomarkers as promising candidates for incorporation into future diagnostic algorithms and therapeutic strategies.

This research lays the groundwork for further exploration into the molecular pathways of gastric cancer progression, ultimately aiming to improve patient outcomes through more accurate risk stratification and timely, targeted interventions.

Acknowledgements

This work was supported by Sanming Project of Medicine in Shenzhen (SZSM202311002); and The Second Batch of Strategic Emerging Industries Support Program of Shenzhen Municipal Development and Reform Commission in 2023 (F-2023-Z99-509269).

Disclosure of conflict of interest

None.

Address correspondence to: Junjie Wan, National Cancer Center/National Clinical Research Center for Cancer/Cancer Hospital & Shenzhen Hospital, Chinese Academy of Medical Sciences and Peking Union Medical College, No. 113 Baohe Road, Longgang District, Shenzhen 518116, China. E-mail: wanjunjie1@163.com

References

[1] Nishimuni M, Claro LCL and Braghiroli MIF. Advancements and challenges in gastric cancer: epidemiology, biomarkers, and therapeutic strategies. Surgical and Experimental Pathology 2024; 7: 19.

[2] Xiang Y and Yao LD. Risk factors for lymph node metastasis and invasion depth in early gastric cancer: analysis of 210 cases. World J Gastrointest Surg 2024; 16: 3720-3728.

[3] Cai F, Dong Y, Wang P, Zhang L, Yang Y, Liu Y, Wang X, Zhang R, Liang H, Sun Y and Deng J. Risk assessment of lymph node metastasis in early gastric cancer: establishment and validation of a seven-point scoring model. Surgery 2022; 171: 1273-1280.

[4] Chen S, Yu Y, Li T, Ruan W, Wang J, Peng Q, Yu Y, Cao T, Xue W, Liu X, Chen Z, Yu J and Fan JB. A novel DNA methylation signature associated with lymph node metastasis status in early gastric cancer. Clin Epigenetics 2022; 14: 18.

[5] Yu M, Zhu L, Dong G, Chen J, Ruan B, Liu Y, Yi S, Meng Z, Chen G, Xu W, Huang J and Han F. Spatiotemporal mapping of lymphatic metastases in gastric cancer using tumor-trackable and enzyme-activatable near-infrared fluorescent nanoprobes. ACS Nano 2024; 18: 35490-35506.

[6] Deng JY and Liang H. Clinical significance of lymph node metastasis in gastric cancer. World J Gastroenterol 2014; 20: 3967-3975.

[7] Díaz Del Arco C, Ortega Medina L, Estrada Muñoz L, García Gómez de Las Heras S and Fernández Aceñero MJ. Pathologic lymph node staging of gastric cancer. Am J Clin Pathol 2021; 156: 749-765.
[8] Zhang Y, Yang P and Wang XF. Microenvironmental regulation of cancer metastasis by miRNAs. Trends Cell Biol 2014; 24: 153-160.
[9] Meng F, Henson R, Wehbe-Janek H, Ghoshal K, Jacob ST and Patel T. MicroRNA-21 regulates expression of the PTEN tumor suppressor gene in human hepatocellular cancer. Gastroenterology 2007; 133: 647-658.
[10] Aalami AH, Aalami F and Sahebkar A. Gastric cancer and circulating micrornas: an updated systematic review and diagnostic meta-analysis. Curr Med Chem 2023; 30: 3798-3814.
[11] Ghafouri-Fard S, Vafaee R, Shoorei H and Taheri M. MicroRNAs in gastric cancer: biomarkers and therapeutic targets. Gene 2020; 757: 144937.
[12] Jahantab MB, Salehi M, Koushki M, Farrokhi Yekta R, Amiri-Dashatan N and Rezaei-Tavirani M. Modelling of miRNA-mRNA network to identify gene signatures with diagnostic and prognostic value in gastric cancer: evidence from in-Silico and in-vitro studies. Rep Biochem Mol Biol 2024; 13: 281-300.
[13] Ouyang J, Xie Z, Lei X, Tang G, Gan R and Yang X. Clinical crosstalk between microRNAs and gastric cancer (review). Int J Oncol 2021; 58: 7.
[14] Roșu MC, Ardelean A, Moldovan SD, Faur FI, Nesiu A and Totoloci BD. The importance of CA 72-4 and CA 19-9 dosing in gastric cancer. J Med Life 2023; 16: 186-188.
[15] Shibata C, Nakano T, Yasumoto A, Mitamura A, Sawada K, Ogawa H, Miura T, Ise I, Takami K, Yamamoto K and Katayose Y. Comparison of CEA and CA19-9 as a predictive factor for recurrence after curative gastrectomy in gastric cancer. BMC Surg 2022; 22: 213.
[16] Zhang S, Li JZ, Du T, Li HQ, Hu RH, Ma CY, Cui XM, Song C and Jiang XH. The modified glasgow prognostic score predicts survival in gastric cancer patients with normal CEA and CA19-9. Can J Gastroenterol Hepatol 2022; 2022: 3953004.
[17] Zhou YC, Zhao HJ and Shen LZ. Preoperative serum CEA and CA19-9 in gastric cancer--a single tertiary hospital study of 1,075 cases. Asian Pac J Cancer Prev 2015; 16: 2685-2691.
[18] Lu C, Lin S, Wen Z, Sun C, Ge Z, Chen W, Li Y, Zhang P, Wu Y, Wang W, Chen S, Zhou H, Li X, Li H, Tao L, Hu Y, Zhao Z, Chen Z, Wu X and Lai Y. Testing the accuracy of a four serum microRNA panel for the detection of primary bladder cancer: a discovery and validation study. Biomarkers 2024; 29: 276-284.
[19] Huang KH, Lan YT, Fang WL, Chen JH, Lo SS, Li AF, Chiou SH, Wu CW and Shyr YM. The correlation between miRNA and lymph node metastasis in gastric cancer. Biomed Res Int 2015; 2015: 543163.
[20] Fan X, Shi C and Lu D. High risk factors related to lymph node metastasis in early gastric cancer: a retrospective observational study. Medicine (Baltimore) 2023; 102: e33431.
[21] Smyth EC, Nilsson M, Grabsch HI, van Grieken NC and Lordick F. Gastric cancer. Lancet 2020; 396: 635-648.
[22] Yang WJ, Zhao HP, Yu Y, Wang JH, Guo L, Liu JY, Pu J and Lv J. Updates on global epidemiology, risk and prognostic factors of gastric cancer. World J Gastroenterol 2023; 29: 2452-2468.
[23] Kim M and Seo AN. Molecular pathology of gastric cancer. J Gastric Cancer 2022; 22: 273-305.
[24] Dou R, Liu K, Yang C, Zheng J, Shi D, Lin X, Wei C, Zhang C, Fang Y, Huang S, Song J, Wang S and Xiong B. EMT-cancer cells-derived exosomal miR-27b-3p promotes circulating tumour cells-mediated metastasis by modulating vascular permeability in colorectal cancer. Clin Transl Med 2021; 11: e595.
[25] Guo T, Tang XH, Gao XY, Zhou Y, Jin B, Deng ZQ, Hu Y, Xing XF, Li ZY and Ji JF. A liquid biopsy signature of circulating exosome-derived mRNAs, miRNAs and lncRNAs predict therapeutic efficacy to neoadjuvant chemotherapy in patients with advanced gastric cancer. Mol Cancer 2022; 21: 216.
[26] Chawra HS, Agarwal M, Mishra A, Chandel SS, Singh RP, Dubey G, Kukreti N and Singh M. MicroRNA-21's role in PTEN suppression and PI3K/AKT activation: implications for cancer biology. Pathol Res Pract 2024; 254: 155091.
[27] Fan MQ, Huang CB, Gu Y, Xiao Y, Sheng JX and Zhong L. Decrease expression of microRNA-20a promotes cancer cell proliferation and predicts poor survival of hepatocellular carcinoma. J Exp Clin Cancer Res 2013; 32: 21.
[28] Ivanovska I, Ball AS, Diaz RL, Magnus JF, Kibukawa M, Schelter JM, Kobayashi SV, Lim L, Burchard J, Jackson AL, Linsley PS and Cleary MA. MicroRNAs in the miR-106b family regulate p21/CDKN1A and promote cell cycle progression. Mol Cell Biol 2008; 28: 2167-2174.
[29] Culcu S, Yuksel C, Aydin F, Bakirarar B, Aksel B and Dogan L. The effect of CEA/Albumin ratio in gastric cancer patient on prognostic factors. Ann Ital Chir 2022; 93: 447-452.
[30] Feng F, Tian Y, Xu G, Liu Z, Liu S, Zheng G, Guo M, Lian X, Fan D and Zhang H. Diagnostic and prognostic value of CEA, CA19-9, AFP and CA125 for early gastric cancer. BMC Cancer 2017; 17: 737.

[31] Li N, Bai C, Zhang R, Ma L, Ren X, Zhang J, Fu Z and Zhao L. Efficacy and safety of apatinib for the treatment of AFP-producing gastric cancer. Transl Oncol 2021; 14: 101004.
[32] Wang YK and Zhang XT. AFP-producing gastric cancer and hepatoid gastric cancer. Zhonghua Zhong Liu Za Zhi 2017; 39: 801-807.
[33] Gong X and Zhang H. Diagnostic and prognostic values of anti-helicobacter pylori antibody combined with serum CA724, CA19-9, and CEA for young patients with early gastric cancer. J Clin Lab Anal 2020; 34: e23268.
[34] Sui X, Zhang Q, Hao M and Chen Y. Serum LINC01133 combined with CEA and CA19-9 contributes to the diagnosis and survival prognosis of gastric cancer. Medicine (Baltimore) 2024; 103: e40564.
[35] Koh SA, Kim MK, Lee KH, Kim SW and Kim JR. RhoGDI2 is associated with HGF-mediated tumor invasion through VEGF in stomach cancer. Clin Exp Metastasis 2014; 31: 805-815.
[36] Si Y, Zhang H, Ning T, Bai M, Wang Y, Yang H, Wang X, Li J, Ying G and Ba Y. miR-26a/b inhibit tumor growth and angiogenesis by targeting the HGF-VEGF axis in gastric carcinoma. Cell Physiol Biochem 2017; 42: 1670-1683.
[37] Xie M, Yu T, Jing X, Ma L, Fan Y, Yang F, Ma P, Jiang H, Wu X, Shu Y and Xu T. Exosomal circSHKBP1 promotes gastric cancer progression via regulating the miR-582-3p/HUR/VEGF axis and suppressing HSP90 degradation. Mol Cancer 2020; 19: 112.
[38] Jiang Y, Huang J, Huang Z, Li W, Tan R, Li T, Chen Z, Tang X, Zhao Y, Qiu J, Li C, Chen H and Yang Z. ADAMTS12 promotes oxaliplatin chemoresistance and angiogenesis in gastric cancer through VEGF upregulation. Cell Signal 2023; 111: 110866.
[39] Dong G, Wang M, Gu G, Li S, Sun X, Li Z, Cai H and Zhu Z. MACC1 and HGF are associated with survival in patients with gastric cancer. Oncol Lett 2018; 15: 3207-3213.
[40] Lodhi MS, Khan MT, Bukhari SMH, Sabir SH, Samra ZQ, Butt H and Akram MS. Probing transferrin receptor overexpression in gastric cancer mice models. ACS Omega 2021; 6: 29893-29904.
[41] Wang X, Yang F, Xu G and Zhong S. The roles of IL-6, IL-8 and IL-10 gene polymorphisms in gastric cancer: a meta-analysis. Cytokine 2018; 111: 230-236.
[42] Dawalibi A, Alosaimi AA and Mohammad KS. Balancing the scales: the dual role of interleukins in bone metastatic microenvironments. Int J Mol Sci 2024; 25: 8163.
[43] Liu M, Li H, Zhang H, Zhou H, Jiao T, Feng M, Na F, Sun M, Zhao M, Xue L and Xu L. RBMS1 promotes gastric cancer metastasis through autocrine IL-6/JAK2/STAT3 signaling. Cell Death Dis 2022; 13: 287.
[44] Liu MC, Oxnard GR, Klein EA, Swanton C and Seiden MV; CCGA Consortium. Sensitive and specific multi-cancer detection and localization using methylation signatures in cell-free DNA. Ann Oncol 2020; 31: 745-759.